EUROPEAN FUSION DEVELOPMENT AGREEMENT

EFDA–JET–CP(01)02-29

B. Esposito, F. Crisanti, P. Maget, V. Parail, Y. Baranov, A. Bécoulet, R.V. Budny,
N. Castaldo, C. D. Challis, R. De Angelis, C. Giroud, N. Hawkes, X. Litaudon,
M. Riva, T. Tala, K.D. Zastrow and JET EFDA Contributors

Correlation Between Magnetic Shear and E×B flow Shearing Rate in JET ITB Discharges

Correlation Between Magnetic Shear and E×B flow Shearing Rate in JET ITB Discharges

B. Esposito[1], F. Crisanti[1], P. Maget[3], V. Parail[2], Y. Baranov[2], A. Bécoulet[3], R.V. Budny[4], N. Castaldo[1], C. D. Challis[2], R. De Angelis[1], C. Giroud[3], N. Hawkes[2], X. Litaudon[3], M. Riva[1], T. Tala[5], K.D. Zastrow[2]
and JET EFDA Contributors*

[1]*Associazione Euratom-ENEA sulla Fusione, C.R. Frascati, C.P. 65, I-00044 Frascati (Roma), Italy*
[2]*Euratom/UKAEA Fusion Association, Culham Science Centre, Abingdon, Oxon. OX14 3DB, UK*
[3]*Association Euratom-CEA sur la fusion, CEA Cadarache, F-13108 Saint Paul-lez-Durance Cedex, France*
[4]*Princeton University Plasma Physics Laboratory, P.O. Box 451, Princeton, New Jersey 08543, USA*
[5]*Association Euratom-Tekes, VTT Chemical Technology, Espoo, Finland*
**See appendix of the paper by J.Pamela "Overview of recent JET results", Proceedings of the IAEA conference on Fusion Energy, Sorrento 2000*

Preprint of Paper to be submitted for publication in Proceedings of the
EPS Conference,
(Maderia, Portugal 18-22 June 2001)

ABSTRACT

The transport reduction in Internal Transport Barrier (ITB) regimes is often correlated with some turbulence suppression. The E×B flow shearing rate is considered to be partially responsible for the decorrelation of the turbulence associated with the Ion Temperature Gradient (ITG) driven modes. However, there are other possible mechanisms, associated with magnetic shear, s, which could explain the onset and characterisation of the ITBs.

From the analysis of various JET discharges having different q profiles (produced by use of LHCD with different timings) and different input momentum (obtained by varying the neutral beam torque), in principle it would be possible to separate the role played by the magnetic shear and the shearing rate. In practice, the difficulties related to the reproducibility of experimental conditions and the data analysis are strongly reducing the above described possibility. Two types of barriers are usually found in JET expriments: barriers at around half radius and more external ones, which are often correlated with some rational q surface.

However, by using a database of selected discharges with available q profiles from EFIT equilibrium reconstruction constrained by Motional Stark Effect (MSE) diagnostic data and limiting the analysis to the inner type barriers, a clear correlation has been found between three different experimental parameters. The location of the foot of the barrier (defined as the position when a critical T_i gradient is achieved) has been compared in space and time with the location of the s=0 curve. It turns that these two quantities seem to coincide within experimental errors. In addition, the ratio between the E×B flow shearing rate, ω_s, and the ITG linear growth rate, γ_η, has also been compared with the previous two quantities. Again, regions with $\omega_s/\gamma_{\eta i}$ >1 are well correlated with the position of both the s=0 curve and the foot of the barrier.

These observed correlations between the magnetic shear, the shearing rate behaviour and the onset of the ITB are tentatively compared with the predictions of theoretical models where the ITG modes are responsible for the anomalous energy transport.

1. EXPERIMENTAL EVIDENCE

A set of about 40 plasma discharges has been studied from year 2000 JET experimental campaign on Internal Transport Barriers (ITBs), by selecting discharges where the q-profiles, as produced by EFIT constrained with Motional Stark Effect (MSE) measurements, were available. The database covers several quite different experimental conditions: with and without LH preheating; with different values of external input of toroidal momentum by using tangential or normal Neutral Beam Injection (NBI) and by varying the fraction of NBI and Ion Cyclotron Heating (ICRH); a large range of total input power; and finally with and without the occurrence of an ITB. All the selected discharges were in H mode.

In most of the discharges where the ITB was present, both the ion and electron temperature profiles are usually showing identical features concerning the location and the timing of the transport barrier, although in few cases the barrier appears on electrons only. Various features characterise the discharges in the database. For instance, the ITB on ions and electrons appears, in different pulses, at different radii. Moreover, in the same pulse, the foot of the barrier is often radially moving outwards with time, sometimes with the appearance of a second ITB. In such a case the first barrier is located around half radius and the second one is in between the first one and the pressure pedestal characterising the H mode.

The appearance of an half-radius barrier is usually linked to the presence of Lower Hybrid Current Drive (LHCD) in the early phase of the discharge (LH preheat). This experimental evidence is by itself a strong indication of a possible important role played by the magnetic shear, s , in the ITB dynamic. The database does not include discharges where an ITB is formed only on the electron temperature profile by using only the LHCD system without any input of toroidal momentum (i.e. NBI).

In Fig.1 it is shown the behaviour of the ion thermal diffusivity (χ_i) as a function of the magnetic shear as obtained from the equilibrium reconstruction code EFIT (conditioned by the MSE data). χ_i has been simply calculated as the ratio of the ion heat flux to $n_e \times \mathrm{grad}(T_i)$. Also by using this transport approach a clear evidence of some interconnection between the magnetic shear and the ITB can be noted. Moreover, the relation between the LHCD preheating and the presence in the discharge of a current density profile with low or negative magnetic shear is clearly demonstrated.

2. THEORY

The most widely accepted explanation for the ITB formation relies on the suppression of Ion Temperature Gradient (ITG) turbulence due to E×B shear flow. The used criterion is that the shearing rate $\omega_s = \omega_s = \left| \frac{RB_\theta}{B_\phi} \frac{\partial}{\partial r}\left(\frac{E_r}{RB_\theta}\right) \right|$ exceeds the ITG linear growth rate $\gamma_{\eta i}$. Here E_r is the radial electric field and B_θ, B_ϕ are respectively the magnetic poloidal and toroidal field. In a previous work [1] a rough analytical expression to estimate $\gamma_{\eta i}$ was used: $\gamma_{\eta i} = k_\theta \rho_s \frac{c_s}{a} f(s) \left(\frac{a}{R}\right)^{1/2} \left(\frac{a}{L_n} + \frac{a}{L_T}\right)^{1/2} \left(\frac{T_i}{T_e}\right)^{1/2}$. L_T, L_n are respectively the typical scale lengths of the ion temperature and density profiles, $c_s = \sqrt{T_e/m_i}$ is the sound speed, $\rho_s = c_s/\Omega$ the sound Larmor radius and k_θ the poloidal wave number. The above formula also contains an explicit dependence on the magnetic shear through the factor f (s); k s is chosen in the range 0.10- 0.15. In [1] f (s) was assumed constant and set to 1. Nevertheless, simulations of the ITG turbulence by Waltz et al. [2] through gyrofluid and gyrokinetic codes show that f (s) has a peak at s ~ 0.5 and decreases at higher and lower values of s. In the following we will discuss whether the inclusion in $\gamma_{\eta i}$ of an explicit dependence on s can lead to a description of all the types of the experimentally observed barriers, by using $\omega_s > \gamma_{\eta i\_Waltz}$ where $\gamma_{\eta i\_Waltz}$ is $\gamma_{\eta i}$ with f (s) as roughly determined by the above simulations (note that for the plasma edge f (s) = f (s = 1) has been used).

An alternative model describing the role of the magnetic shear in the barrier formation is given in Hamaguchi and Horton [3], where the linear stability theory parameter $Y_s = \sqrt{\frac{m_i}{T_e}} \left| \frac{R\partial_\psi\left(\frac{Er}{RB_\theta}\right)}{\partial_\psi \ln q} \right|$ is introduced: the ITG-driven turbulence is significantly reduced when Y_s nexceeds a given critical value $Y_c = 2\ Y_s = 2\sqrt{\frac{(1+\eta_i)\,T_i}{T_e}}$, where $\eta_i = L_n/L_T$. Of course, given the dependence on s , this criterion is always satisfied close to the s = 0 surface. A cross check with experimental data will be also carried out in this framework.

3. COMPARISON BETWEEN THEORY AND EXPERIMENT

Figure 2 shows the radial evolution of T_i, ω_s, $\gamma_{\eta i}$ and $\gamma_{\eta i\_Waltz}$ for Pulse No: 51572 (I_p = 2.2MA, B_t = 2.6 T, NBI + ICRH = 17MW) at 4 subsequent times; 1.6MW of LHCD were applied during the current ramp-up, and consequently the q-profile was hollow all along the pulse. It can be noted that when s is compared with $\gamma_{\eta i\_Waltz}$ the formation and time evolution of two barriers is well described by the $\omega_s > \gamma_{\eta i\_Waltz}$ criterion: a barrier forms early at R ~ 3.4m (where $\omega_s > \gamma_{\eta i\_Waltz}$ at t = 4.7-5.9s) and a second one appears later for t = 6.2s (again $\omega_s > \gamma_{\eta i\_Waltz}$) at R ~ 3.6 m. On the contrary, using the evaluation of the growth rate without the explicit dependence on the magnetic shear (i) the dynamics of the double barrier cannot be described.

For the same discharge, in Fig.3, is given the location of the s = 0 surface versus time, together with the barrier location in both electron and ion temperature profiles as determined by a dimensionless ITB criterion based on $\rho_T^* \geq \rho^*_{ITB} = 1.4\times10^{-2}$, where $\rho_T^* = \rho_s/L_T$ is the local dimensionless Larmor radius [4]. Note that ρ_T^* refers just to one barrier at a time (the strongest). It can be seen that a correlation between barrier location and s = 0 is possible, although none of the two barriers is strictly related with the s = 0 position. The double barrier formation cannot be explained by the Hamaguchi and Horton approach, since Y_s exceeds Y_c at the same radial location (Fig.4) throughout the discharge (see Fig.3 where the location of s = 0 remains unchanged); such approach also is not working for discharges with barriers and monotonic q-profiles, although it could explain half-radius barriers with reversed q-profiles.

Further results are shown for Pulse No: 51573 (similar to the Pulse No: 51572 and with 16.3MW of NBI + ICRH) where a single central barrier appears at t = 5.6 s and evolves slightly outwards, consistently with the results of JETTO code transport calculations in interpretative mode (Fig.5): the region where the i remains low (of the order of the neoclassical value) is expanding in time together with the region where s > $\gamma_{\eta i\_Waltz}$.

CONCLUSIONS

It appears that by taking into account the "correct" dependence on the magnetic shear in the linear growth rate evaluation, as given by gyrokinetic and gyrofluid codes [2], it is qualitatively possible to explain the radial location, the time of formation and the time evolution of different kinds of transport barriers in terms of the widely accepted mechanism based on the E×B shear flow suppression of ITG-driven electrostatic turbulence. This is true for almost all the discharges of the selected database, except for few discharges where the picture is not completely clear, either due to experimental errors or to the presence of an additional/alternative mechanism of turbulence suppression.

For instance, Fig.6 refers to a barrier appearing only on electron temperature profiles (Pulse No:

51446: $I_p = 2.2$MA, $B_t = 2.6$T): this is shown by the fact that ρ_{T_e}* satisfies the ITB criterion, while the equivalent quantity for the ions, ρ_{T_i}*, practically always remains below threshold. In the chosen time interval the q-profile is reversed (2.1 MW of LHCD preheating) and the total (NBI+ICRH) additional power is high (~16 MW). Such behaviour could be explained if these T_e only barriers are produced by a different stabilisation mechanism: for example, the short wavelength ETG turbulence might be stabilised by the negative magnetic shear, while the input of the external momentum by the NBI is not enough to trigger the ITG stabilisation mechanism. Another possibility could be that the underlying turbulence is of different nature (electromagnetic instead of electrostatic).

REFERENCES

[1] F. Crisanti, B. Esposito, C. Gormezano et al., in press, Nucl. Fus. (2001)
[2] R.E. Waltz, G.M. Staebler, W. Dorland et al., Phys. Plasmas **4**, 2482, (1997)
[3] S. Hamaguchi and W. Horton, Phys. Fluids **B4**, 319, (1992)
[4] G. Tresset, X. Litaudon, D. Moreau, Report EUR-CEA-FC-1700, (2000)

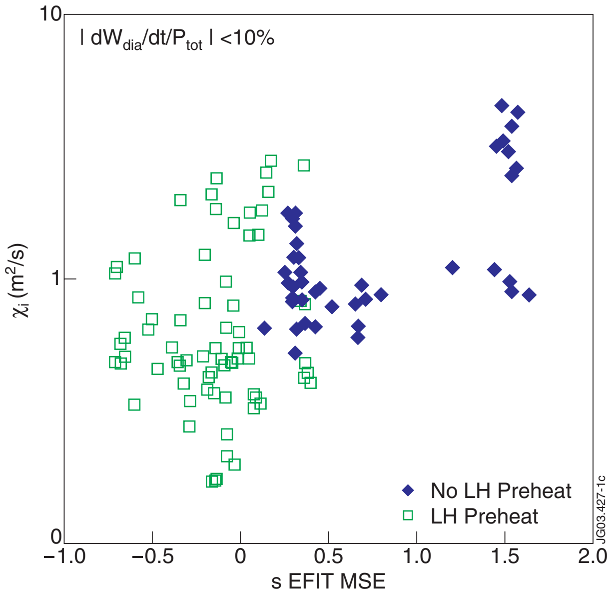

Figure 1: Ion diffusivity evaluated for all discharges in the database.

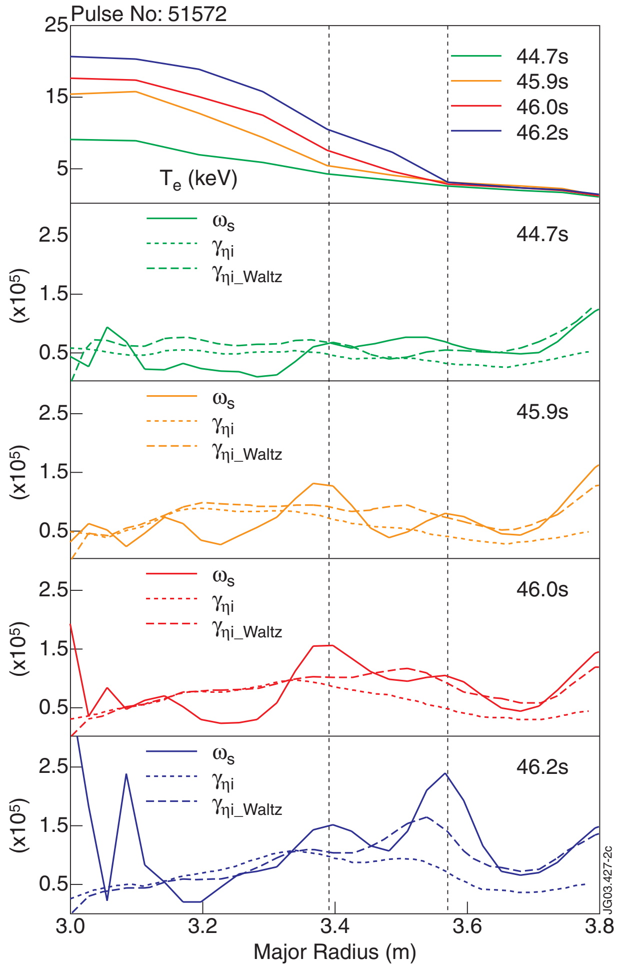

Figure 2: Shearing rate and linear growth rate (with f(s)=1 and f(s) as in Waltz [2]) at subsequent times in Pulse No: 51572 (units s^{-1}); T_i profiles are also plotted.

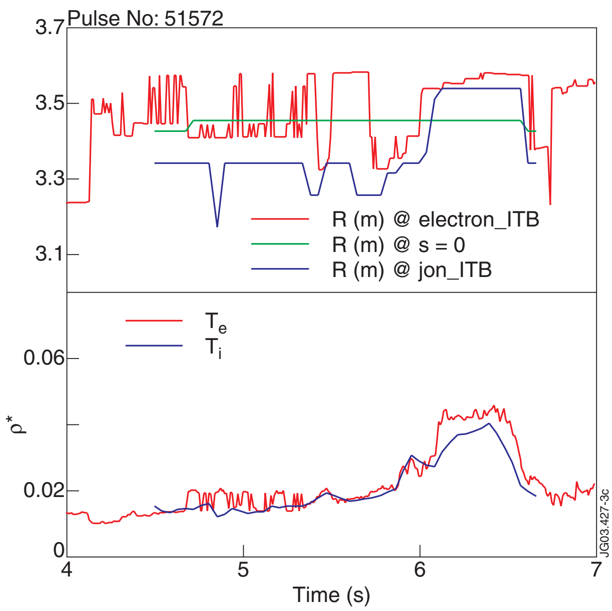

Figure 3: Location of T_e, T_i barriers and s=0 curve (top); ITB criterion [4] for electrons and ions (bottom).

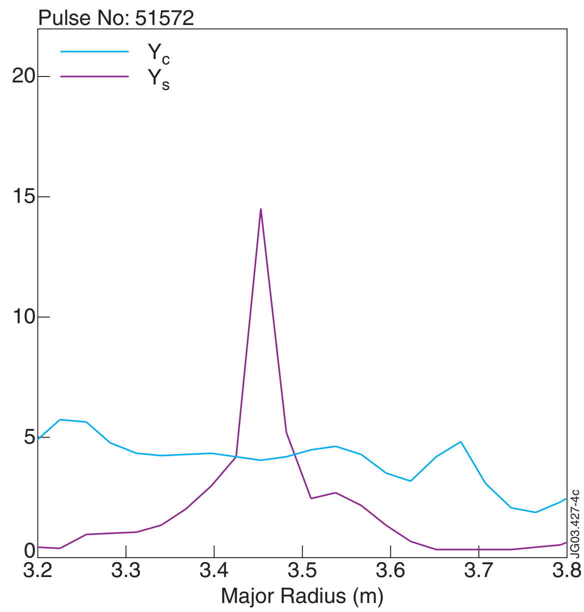

Figure 4: Showing the Hamaguchi-Horton parameter (Y_s) and its critical value (Y_c) for Pulse No: 51572 at t = 6.4s

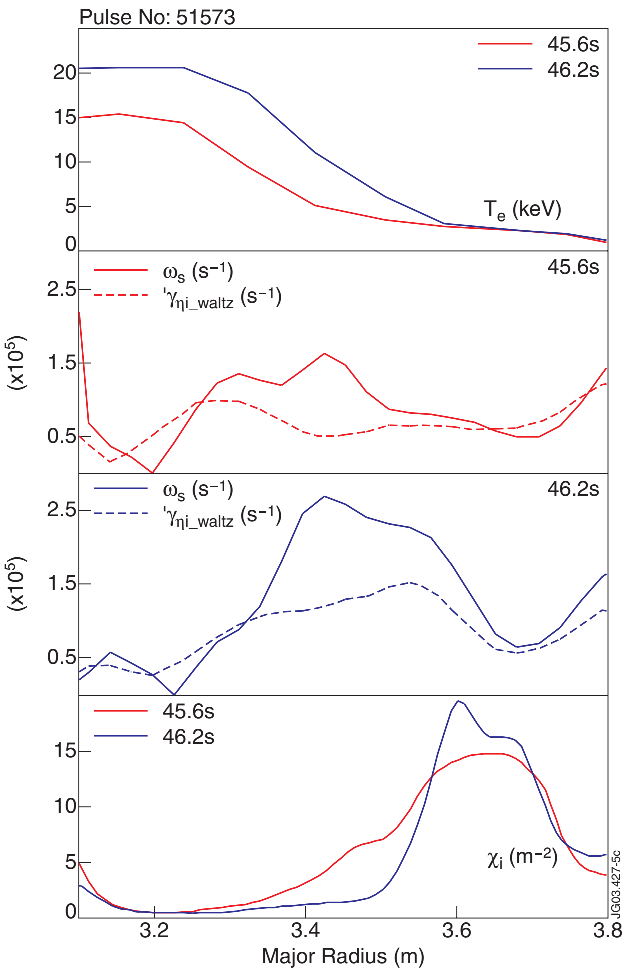

Figure 5: Ti, shearing rate, linear growth rate (with f(s) as in Waltz [2]) and calculated χ_i for Pulse No: 51573.

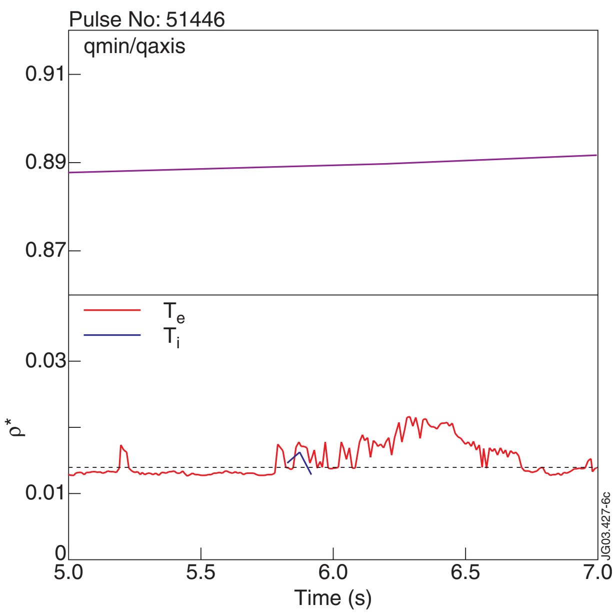

Figure 6: Pulse No: 51446: ratio q_{min}/q_{axis} versus time (top); ITB criterion [4] for electrons and ions (bottom).